Generic modelling of cooperative growth patterns in bacterial colonies

Eshel Ben-Jacob*, Ofer Schochet*, Adam Tenenbaum*, Inon Cohen*, Andras Czirók† & Tamas Vicsek†

School of Physics and Astronomy,
Raymond & Beverly Sackler Faculty of Exact Sciences,
Tel-Aviv University, Tel-Aviv 69978, Israel
† Department of Atomic Physics, Eötvös University, Budapest,
Puskin u5-7, 1088 Hungary

BACTERIAL colonies must often cope with unfavourable environmental conditions[1,2]. To do so, they have developed sophisticated modes of cooperative behaviour[3–10]. It has been found that such behaviour can cause bacterial colonies to exhibit complex growth patterns similar to those observed during non-equilibrium growth processes in non-living systems[11]; some of the qualitative features of the latter may be invoked to account for the complex patterns of bacterial growth[12–18]. Here we show that a simple model of bacterial growth can reproduce the salient features of the observed growth patterns. The model incorporates random walkers, representing aggregates of bacteria, which move in response to gradients in nutrient concentration and communicate with each other by means of chemotactic 'feedback'. These simple features allow the colony to respond efficiently to adverse growth conditions, and generate self-organization over a wide range of length scales.

We have grown bacterial colonies under different growth conditions[12,13] ranging from a very low level of nutrient (0.1 g peptone per litre) to a very rich mixture (10 g peptone per litre), and from a soft substrate (~1% agar concentration) to a hard substrate (4% agar concentration). Growth was started with a droplet (5 μl containing $\sim 10^5$ bacteria) inoculation at the centre of Petri dishes incubated at 37 °C and 30% humidity. The growth pattern we describe are of bacteria derived from *Bacillus subtilis* strain 168 (refs 12, 13). The colonies adopt various shapes as growth conditions are varied (Fig. 1): patterns are compact at high peptone concentrations and become more ramified at low peptone concentrations (0.5 g l^{-1}), in agreement with results reported in refs 12–18. Surprisingly, at $< \sim 0.25$ g peptone per litre, colonies adopt a more organized (well defined circular envelope), dense structure (Fig. 1*d*).

Optical microscopy reveals that the bacteria perform a random walk-like movement within a well defined envelope. The latter (Fig. 2) is formed presumably by chemicals that are excreted by the bacteria and/or by fluid drawn by the bacteria from the agar. The envelope propagates slowly as if by the action of effective internal pressure produced by the collective movement of the bacteria. At very low peptone concentrations the density of bacteria is low—the distance between bacteria is up to several times the size of an individual bacterium. In this range, the bacteria are longer (~5 μm) (Fig. 2*e*) and the movement seems to be more organized. At high agar concentration there is a boundary layer of high bacterial density at the leading tips of the growing branches (Fig. 2*f*). In this range, colonies display a pronounced structure in the perpendicular direction as well (Fig. 2*c*).

The growth of bacterial colonies presents an inherent additional level of complexity compared to non-living systems, as the building blocks themselves are living systems[15,19,20], each having its own autonomous (at times 'selfish') self-interest and internal degrees of freedom. To model the growth, we included the following generic features: (1) diffusion of nutrients; (2) movement of the bacteria; (3) reproduction and sporulation; (4) local communication. Diffusion of nutrients is handled by solving the

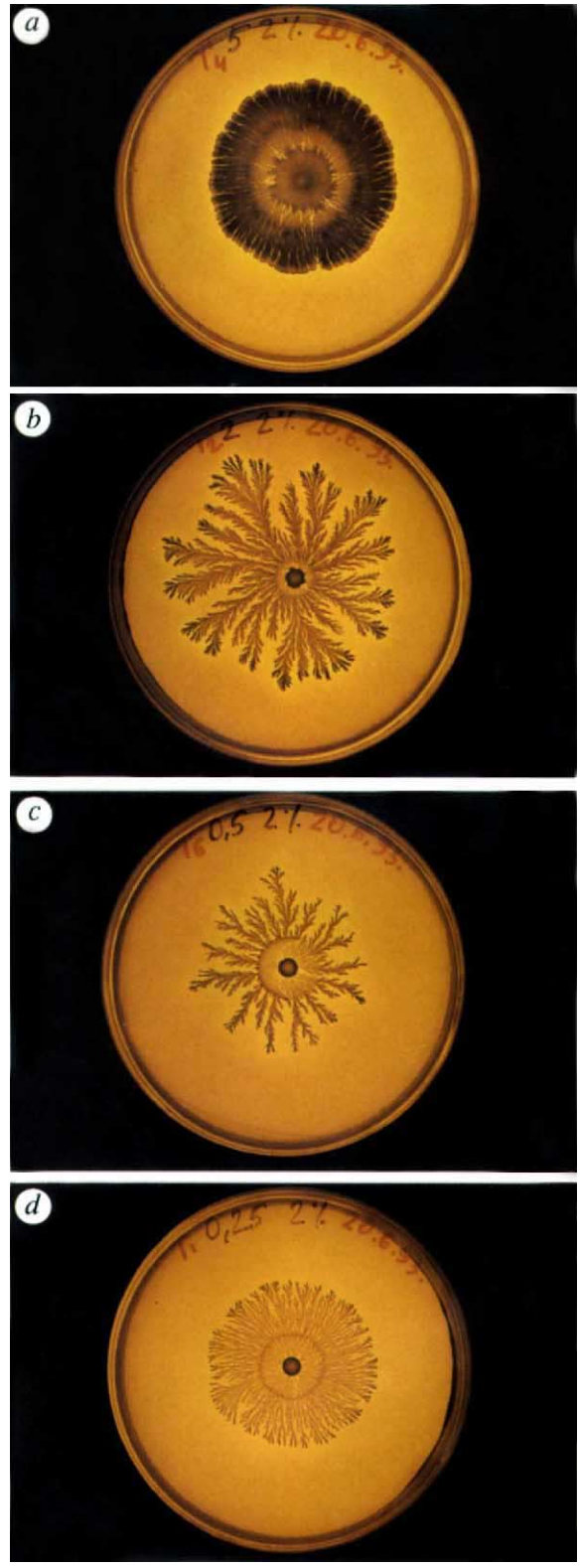

FIG. 1 Observed patterns of colonies grown on a substrate with 2% agar concentration. The peptone level is 5, 2, 0.5 and 0.25 g l^{-1} for *a*, *b*, *c* and *d* respectively. At high peptone levels the branches are wide, the pattern is very reminiscent of Hele–Shaw patterns[11] and the fractal dimension is close to two. As the peptone level is decreased, the patterns become more ramified (*b* and *c*), reminiscent of patterns observed during electrochemical deposition[11] (*b*) and diffusion limited aggregation (DLA)[22] simulations (*c*). At even lower peptone levels the patterns become denser again (*d*). As explained in the text, we expect this phenomenon to result from chemotaxis signalling.

© 1994 Nature Publishing Group

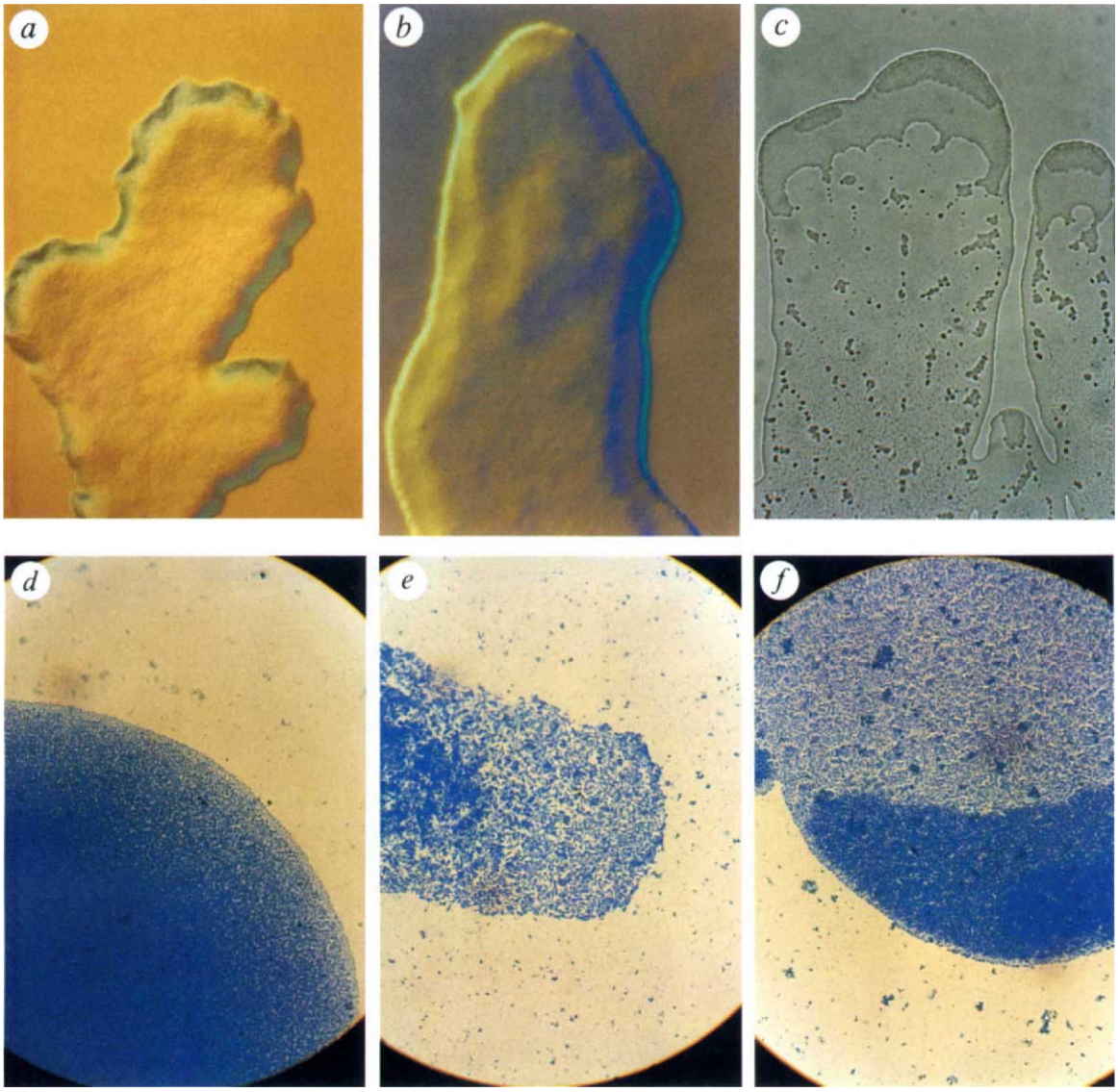

FIG. 2 Optical microscope observations of the colonies. *a* and *b*, Using a Numarski prism to indicate the sharpness of the envelopes. In *a* the envelope is rougher in the horizontal direction. *c*, Using transmitted light to show the complex three-dimensional structure of growth on substrates with a high agar concentration (2.5%). *d*, *e*, *f*, Micrographs of stained colonies. *d*, Intermediate values of peptone level and agar concentration. *e*, Low peptone level. *f*, High agar concentration: note the higher bacteria density at the tip in this case. Magnifications: *a*, *b*, *c*, ×28; *d*, *e*, *f*, ×280.

diffusion equation for the nutrient concentration c on a triangular lattice. The bacteria are represented by walkers, each of which should be viewed as a mesoscopic unit (coarse graining of the colony) and not as an individual bacterium.

Each walker is described by its location $\vec{r}_i$ and an internal degree of freedom ('internal energy' W_i), which affects its activity. The walker loses 'internal energy' at a rate e. To increase the internal energy it consumes nutrients at a fixed rate c_r, if sufficient food is available. Otherwise, it consumes the available amount. When there is not enough food for an interval of time (causing W_i to drop to zero), the walker becomes stationary (sporulation). When food is sufficient, W_i increases, and when it reaches some threshold t_r, the walker divides into two (reproduction).

The walkers perform off-lattice random walk within a well defined envelope (defined on the triangular lattice in Fig. 3*a*). Each segment of the envelope moves after it has been hit N_c times by the walkers. This requirement represents the local communication or cooperation in the behaviour of the bacteria. Note that, to a first approximation, the level of N_c represents the agar concentration, as more 'collisions' are needed to push the envelope on a harder substrate.

The model equations are:

$$\frac{\partial c(\vec{r}, t)}{\partial t} = D_c \nabla^2 c(\vec{r}, t) - \sum_{\text{active walkers}} \delta(\vec{r} - \vec{r}_i) \min (c_r, c(\vec{r}, t)) \quad (1)$$

This is the diffusion equation for the nutrients (D_c is the diffusion constant) which includes the consumption of food by the walkers (last term). The time evolution of W_i is given by:

$$\frac{dW_i}{dt} = \min (c_r, c(\vec{r}_i, t)) - e \quad (2)$$

At each time step, each of the active random walkers performs a random walk of step size d at an angle Θ, uniformly chosen from the interval $[0, 2\pi]$. Thus the new location $\vec{r}_i'$ is given by:

$$\vec{r}_i' = \vec{r}_i + d(\cos \Theta, \sin \Theta) \quad (3)$$

If the step $\vec{r}_i \rightarrow \vec{r}_i'$ crosses the envelope, the step is not performed and a counter on the appropriate segment of the envelope is

© 1994 Nature Publishing Group

increased by one. When a segment counter reaches N_c, the envelope segment is shifted by one lattice step.

Results of numerical simulations of the model are shown in Fig. 3*b*. As in the growth of bacterial colonies, the patterns are compact at high peptone levels and become fractal with decreasing food level. For a given peptone level, the patterns are more ramified as the agar concentration increases. Clearly, the results shown in Fig. 3 are very encouraging and do capture features of the observed patterns. However, there are some crucial qualitative differences. The most dramatic one is the ability of the bacteria to develop organized patterns at very low peptone levels (Fig. 1*d*), a feature which is not captured by this version of the model.

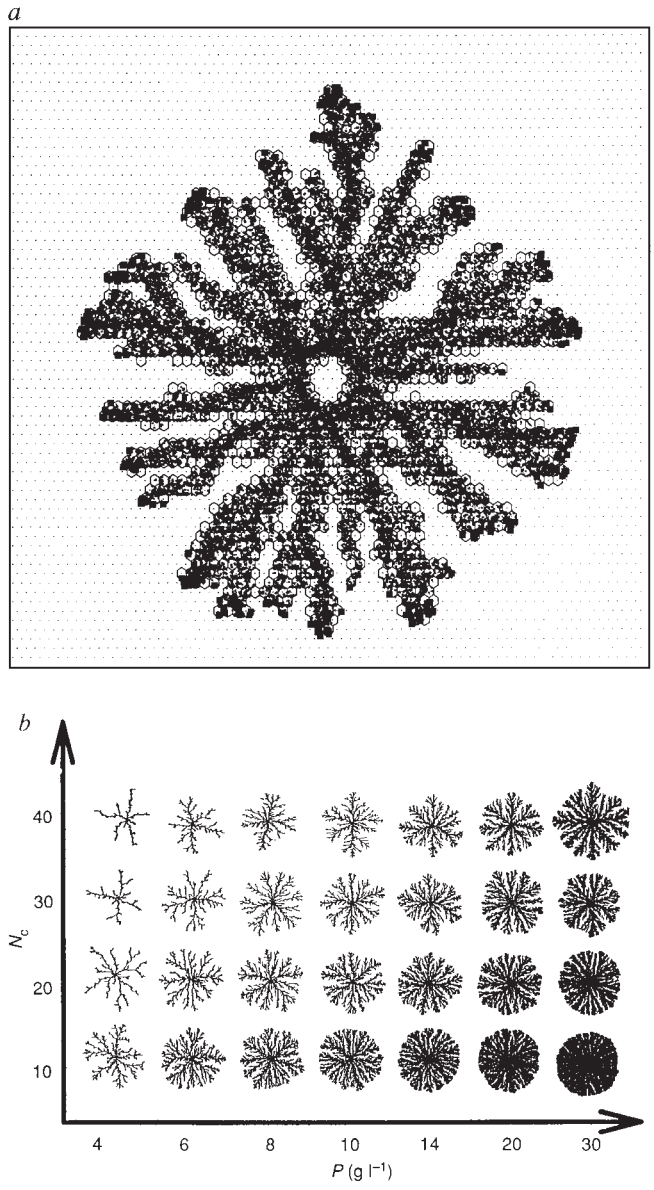

FIG. 3 The communicating walkers model. *a*, Close-up view of the model. The solid squares are the active walkers and the heavy dots are the stationary ones. Equation (1) is solved on the underlying triangular lattice. The hexagons mark the envelope. *b*, Results of numerical simulations of the communicating walkers model. The patterns are organized as function of peptone level P (the initial value of c) and N_c (corresponds to the agar concentration). The typical system size is 600×600 and the typical number of the walkers is 10^5. Hence each walker represents $\sim 10^4$ bacteria. The observed patterns are compact for high peptone levels and become ramified for low peptone levels. For the same peptone level, the patterns are more branched for higher N_c. Both are consistent with experimental observations. Note that the fractal dimension becomes much smaller than the DLA fractal dimension[22]. It reflects the fact that the envelope propagation has non-trivial dependence on the gradient of the nutrients diffusion field.

As the environmental conditions become more hostile (low peptone concentration or hard surface), a higher level of cooperation is required for a more efficient response of the colony. Non-local communication and transfer of information between each of the individuals and the colony might be needed. Can chemotactic signalling provide the colony with the means to do so? Generally, chemotaxis means movement of the microorganisms in response to a concentration gradient of certain chemicals[6,10]. Ordinarily, the movement is along the gradient, either in the direction of the gradient or the opposite direction. The chemotactic response may be to an external chemical field or to one produced by the microorganisms; the latter may be called chemotactic signalling or communication. Moreover, it is well known[4] that excretion of the signal can be triggered by an external stress. Such non-local communication enables each bacterium to obtain information about the state of the colony as a whole and to respond to it. For example, the migration of *Dictyostelium* under low nutrient conditions depends on chemotactic signalling via cyclic adenosine monophosphate (cAMP)[21]. In this case, each of the microoooorganisms may excrete and consume cAMP and move according to its concentration gradient.

Here we include a simple version of chemotactic communication in the hope of identifying the generic features that it induces. Each of the stationary walkers (or alternatively, walkers which have been exposed to a low level of food) produces a communication chemical at a fixed rate s_r (in an attempt to drive other bacteria away), and each of the active walkers consumes the chemical at a fixed rate c_c. As we show below, this simplified version is sufficient to capture the qualitative features of the growth. A more realistic model would include a dependence of these rates on the concentrations of nutrients and chemotactic signalling compounds. The equation of the communication field in the present model is given by:

$$\frac{\partial s(\vec{r}, t)}{\partial t} = D_s \nabla^2(\vec{r}, t) + \sum_{\text{stationary walkers}} \delta(\vec{r} - \vec{r}_i) s_r - \sum_{\text{active walkers}} \delta(\vec{r} - \vec{r}_i) \min(c_c, s(\vec{r}, t)) \quad (4)$$

The movement of the active bacteria changes from pure random walk (equal probability to move along any direction) to a random walk with a bias along the gradient of the communication field (high probability to move in the direction of the signalling material).

In Fig. 4 we show that the inclusion of such chemotaxis signalling indeed produces the desired phenomena. The pattern

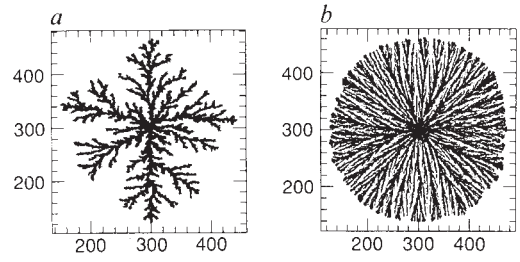

FIG. 4 Effect of chemotaxis signalling on the communicating walkers model. *a*, In the absence of the chemotaxis for $P = 10$ g l^{-1} and $N_c = 40$. *b*, In the presence of chemotaxis (for the same values of P and N_c). The pattern becomes denser with radial thin branches and well defined circular envelope, in aggreement with experimental observations. The numbers on the axes represent the trigonal lattice sites to indicate the system size.

© 1994 Nature Publishing Group

changes from fractal to a dense structure with thin branches and a well defined circular envelope. Moreover, the number of walkers (bacteria density) in the colony is much lower than in the absence of chemotaxis. We find that a chemotactic response to gradients of nutrient concentration does not reproduce this effect. Here we have simply introduced chemotactic signalling when the peptone level becomes low; in reality, there might be additional control mechanisms which change the intensity of the chemotaxis communication as the bacteria go through phenotypic transformations. We suspect that the observed perpendicular growth at high agar concentration also results from chemotactic signalling.

Our goal in this work is to demonstrate that apparently complex behaviour in biological systems can be elucidated by relatively simple, generic modelling in conjunction with a close comparison to experimental observations. □

Received 19 August; accepted 21 December 1993.

1. Stainer, R. Y., Doudoroff, M. & Adelberg, E. A. *The Microbial World* (Prentice-Hall, New Jersey, 1957).
2. Shapiro, J. A. *Scientific American* **258** (6) 62–69 (1988).
3. Shapiro, J. A. & Trubatch, D. *Physica* D**49,** 214–223 (1991).
4. Budrene, E. O. & Berg, H. C. *Nature* **349,** 630–633 (1991).
5. Kessler, J. O. *Contemp. Phys.* **26,** 147–166 (1985).
6. Adler, J. *Science* **166,** 1588–1597 (1969).
7. Lackiie, J. M. (ed.) *Biology of the Chemotactic Response* (Cambridge Univ. Press, 1981).
8. Devreotes, P. *Science* **245,** 1054–1058 (1989).
9. Berg, H. C. & Purcell, E. M. *Biophys. J.* **20,** 193–219 (1977).
10. Nossal, R. *Expl Cell Res.* **75,** 138–142 (1972).
11. Ben-Jacob, E. & Garik, P. *Nature* **343,** 523–530 (1990).
12. Ben-Jacob, E., Shmueli, H., Shochet, O. & Tenenbaum, A. *Physica* A**187,** 378–424 (1992).
13. Ben-Jacob, E., Tenenbaum, A., Shochet, O. & Avidan, O. *Physica* A**202,** 1–47 (1994).
14. Henrici, T. H. *The Biology of Bacteria* 3rd edn (Heath, Boston, 1948).
15. Cooper, A. L. *Proc. R. Soc.* B **171,** 175–199 (1968).
16. Fujikawa, H. & Matsushita, M. *J. phys. Soc. Japan* **58,** 3875–3878 (1989).
17. Matsuyama, T. & Matsushita, M. *Crit. Rev. Bact.* **19,** 117–135 (1993).
18. Schindler, J. & Rataj, T. *Binary* **4,** 66–72 (1992).
19. Allison, C. & Hughes, C. *Sci. Prog.* **75,** 403–422 (1991).
20. Henrichsen, J. *Bacter. Rev.* **36,** 478–503 (1972).
21. Kessler, D. & Levine, H. *Phys. Rev.* E (in the press).
22. Sander, L. M. *Nature* **322,** 789–795 (1986).

ACKNOWLEDGEMENTS. We thank I. Brainis, D. Weiss and H. Leibovich for technical assistance. We have benefited from conversations with J. Shapiro, E. Ron, D. Gutnik, D. Kessler, H. Levine and P. Garik. This research was supported in part by the German–Israeli Foundation for Scientific Research and Development, the Hungarian Research Foundation and the Program for Alternative Thinking at Tel-Aviv University.

Productivity of pre-vascular continental biota inferred from the $Fe(CO_3)OH$ content of goethite

Crayton J. Yapp & Harald Poths

Department of Earth and Planetary Sciences,
University of New Mexico, Albuquerque, New Mexico 87131, USA

CHEMICAL weathering of rocks by CO_2—an important process in the carbon cycle—may have been affected by the appearance of vascular plants during the Silurian period (438–408 Myr ago), because of the enhanced efficacy of these plants in promoting weathering[1]. The magnitude of this effect is uncertain, however[2–4]. One key issue is the concentration of CO_2 in soils, generated by microbial respiration; this is itself in part a function of soil productivity. We showed recently[5] that the CO_2 partial pressure in a Late Ordovician soil was 5.6 times that in the atmosphere; Keller and Wood[6] have shown, however, that soil CO_2 concentrations can be high even for low levels of microbial respiration, as a result of slow diffusion of respired CO_2 out of the soil. Here we present an analysis of the $Fe(CO_3)OH$ component of goethite (FeOOH) in an Upper Ordovician oolitic ironstone which underwent tropical chemical weathering 440 Myr ago[7,8]. These data allow us to extract an estimate of the CO_2 flux from the soil profile. The high rate that we obtain implies that the productivity of pre-vascular biota was similar to that in modern soils. Thus, attempts to model atmospheric CO_2 concentrations over Phanerozoic[9–12] time need not assume that pronounced productivity changes accompanied the development of vascular plants.

The common mineral goethite (α-FeOOH) contains an $Fe(CO_3)OH$ component in apparent solid solution[13–15]. The abundance and $^{13}C/^{12}C$ ratio of this component seem to be a measure of the partial pressure (p_{CO_2}) and carbon isotope ratio, respectively, of CO_2 present at the time of goethite crystallization. The Upper Ordovician Neda Formation at its type locality near Neda, Wisconsin, USA, is a goethite-dominated, oolitic ironstone whose upper surface is a Late Ordovician unconformity[7]. The goethite in this ironstone has apparently remained a closed system since the time of its formation in the Late Ordovician ~440 Myr ago[5,8,16]. A subaerial weathering origin for this ancient goethite at a temperature of ~23 °C is supported by the existence of the unconformity[7], by oxygen isotope data which indicate the presence of meteoric water ($\delta^{18}O = -7.3$) at the time of crystallization[8], and by the vertical distribution of the carbon isotope and mole fraction data of the $Fe(CO_3)OH$ component[17]. The measured mole fractions (X) of the $Fe(CO_3)OH$ component in different Neda Formation goethite samples are plotted as a function of sample depth below the unconformity in Fig. 1*a*. These data are tabulated in ref. 5. Values of X increase relatively rapidly from the unconformity to a depth of ~30 cm. The changes in X are more gradual at greater depths. If the changes in X in Fig. 1*a* reflect variations in ancient ambient p_{CO_2}, the indicated pattern is generally con-

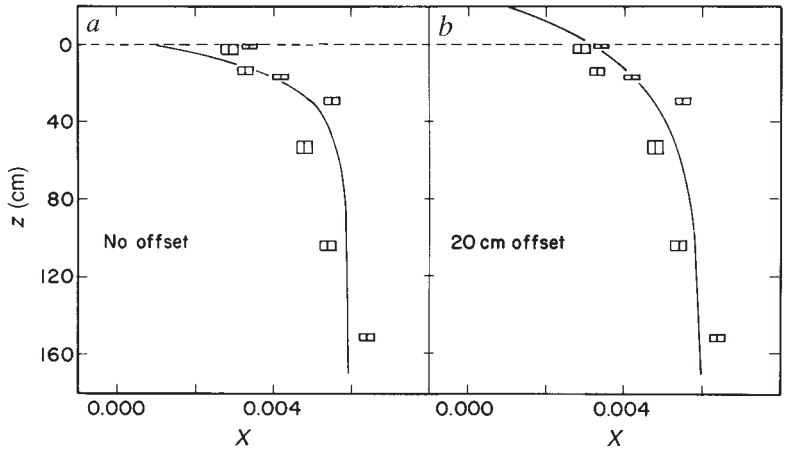

FIG. 1 *a*, *b*, Mole fractions (X) of the $Fe(CO_3)OH$ component in goethite of the Neda Formation oolitic ironstone plotted as a function of sample depth (z) below the unconformity that defines the top of the deposit (the dashed line at $z = 0$). The width of each data symbol represents the analytical uncertainty of $\sim \pm 0.0002$ for values of X. The height of each symbol corresponds to the vertical interval represented by the sample. These data are tabulated in ref. 5. The curved lines represent model calculations for one-dimensional steady-state, diffusive transport of CO_2 in a soil profile (see text). The calculated model curve in *a* assumes that the existing unconformity corresponds to the original weathering surface (no offset). The curve in *b* was calculated assuming that 20 cm of the deposit were eroded ($z + 20$) before the deposit was buried beneath Early Silurian marine carbonates (see text).

© 1994 Nature Publishing Group